Available online at www.sciencedirect.com
SCIENCE DIRECT®
Computers and Structures 83 (2005) 1386–1395
Computers & Structures
www.elsevier.com/locate/compstruc

Coupling and enrichment schemes for finite element and finite sphere discretizations

Jung-Wuk Hong, Klaus-Jürgen Bathe *

Department of Mechanical Engineering, Massachusetts Institute of Technology, 77 Massachusetts Avenue, Room 3-356, Cambridge MA 02139, United States

Accepted 12 October 2004
Available online 13 March 2005

Abstract

We present a technique to couple finite element and finite sphere discretizations. The finite elements and finite spheres are coupled with full displacement compatibility. We also present a technique in which a finite element discretization is enriched with finite spheres. We consider two-dimensional conditions and present solutions to illustrate the analysis procedures.

1. Introduction

For several decades, the development of the finite element method has been pursued and the method is now quite efficient for the analysis of complex structures and, indeed, many quite general multi-physics problems [1,2]. However, the finite element method requires an expensive mesh generation and, in some cases, notably in nonlinear analysis, mesh re-generations may be necessary. On the other hand, meshless techniques eliminate the mesh generation procedure in the analysis, but are confronting difficulties in numerical integration; namely, the integrands are very complex functions. Also, the essential boundary conditions are not as easily imposed as in the traditional finite element method. To overcome these difficulties, some research focused on coupling finite element methods and meshless techniques [3–5], with the premise to utilize the mutual advantages. The basic idea is that finite elements are employed for the domain which is easily meshed and would not need re-meshing in a geometrically nonlinear analysis, and the meshless discretizations are used for the domain which is difficult to mesh and may need re-meshing in nonlinear analysis. However, a major difficulty lies in enforcing compatibility in the displacements as assumed for the meshless domain and the finite element domain: that is, to ensure the continuity of the displacements and possibly displacement derivatives between the domains. Although some methods for coupling were proposed, full displacement compatibility in the coupled domain seems not ensured. In this paper, we propose a displacement-based scheme to couple finite elements and finite spheres [6–8]. We consider two-dimensional analysis, the four-node displacement-based finite element in the coupling with finite spheres, and we achieve in the formulation continuity of the displacements in the domain of overlap.

We also propose a procedure to simply enrich the displacement interpolation in the finite element domain. In this method, finite sphere interpolations are added to the

* Corresponding author. Tel.: +1 617 253 6645; fax: +1 617 253 2275.
E-mail address: kjb@mit.edu (K.J. Bathe).

0045-7949/$ - see front matter © 2005 Elsevier Ltd. All rights reserved.
doi:10.1016/j.compstruc.2004.12.002

existing finite element interpolations. Of course, schemes to enrich finite element interpolations (and enrich other bases by finite elements) have been used for a long time [9], but the approach presented here provides particular flexibility since it is possible to add or remove spheres adaptively. The spheres can be added only in local areas of the entire analysis domain with no restriction on the geometry analyzed and finite element mesh used.

There are many promising application areas, even when considering only linear analysis. Regions that are difficult to mesh with finite elements can be modelled more easily and regions of stress concentrations can, possibly, be analyzed more effectively. In the following sections of the paper, we present the theory of the coupling and enriching schemes and illustrate their use in various example solutions.

2. Coupling finite element and finite sphere discretizations

In the formulation to couple finite element and finite sphere discretizations, we need to categorize the regions in the complete domain considered, and construct the shape functions.

Let Ω be the complete domain considered, Γ_u its surface area on which displacements are prescribed and Γ_f its surface area on which tractions are prescribed. Also, let $\Omega_{\mathrm{FE}}^{(k)}$ be the domain of the finite element (k), $k = 1, \ldots, N_{\mathrm{fe}}$, and let $\Omega_{\mathrm{FS}}^{(k)}$ be the domain of the finite sphere (k), $k = 1, \ldots, N_{\mathrm{fs}}$, with N_{fe} and N_{fs} being the total number of finite elements and finite spheres. We then further define

$$\Omega_{\mathrm{FE}} = \left\{ \cup \Omega_{\mathrm{FE}}^{(k)}; \quad \Omega_{\mathrm{FE}}^{(k)} \cap \Omega_{\mathrm{FS}}^{(j)} = 0, \quad \text{all } j \right\}, \tag{1}$$

$$\Omega_{\mathrm{FE-FS}} = \left\{ \cup \Omega_{\mathrm{FE}}^{(k)}; \quad \Omega_{\mathrm{FE}}^{(k)} \cap \Omega_{\mathrm{FS}}^{(j)} \neq 0, \quad \text{some } j \right\}, \tag{2}$$

$$\Omega_{\mathrm{FS}} = \{ \Omega \setminus (\Omega_{\mathrm{FE}} \cup \Omega_{\mathrm{FE-FS}}) \}. \tag{3}$$

Consider a simple example, as illustrated in Fig. 1. We have a total of $N_{\mathrm{fe}} = 6$ finite elements and $N_{\mathrm{fs}} = 9$ finite spheres, which overlap in the "coupled" domain. According to Eqs. (1)–(3) we categorize the complete domain considered into three different domains. We call Ω_{FE} the domain discretized using finite elements only, i.e, the domain which does not overlap with finite spheres, $\Omega_{\mathrm{FE-FS}}$ the coupled domain, i.e, the union of finite elements that overlap with spheres, and Ω_{FS} the pure finite sphere domain, i.e, the domain which is represented by spheres only.

With these definitions from here on, the domain $\{\Omega_{\mathrm{FE}}^{(k)}, k \in \mathscr{M}\}$ shall denote a pure finite element subdomain, $\{\Omega_{\mathrm{FE-FS}}^{(k)}, k \in \mathscr{N}\}$ shall denote a finite element subdomain coupled with at least one sphere, and $\{\Omega_{\mathrm{FS}}^{(k)}, k \in \mathscr{S}\}$ shall denote a pure sphere subdomain over which we integrate, see Fig. 1. Note that with these definitions the union of the subdomains comprises the complete domain Ω.

Of course, the displacements in the complete domain are formed by the displacement interpolations. The complete nodal coefficient vector of unknown values corresponds to all degrees of freedom of the finite elements and the finite spheres

$$\mathbf{U}^{\mathrm{T}} = [\mathbf{u}_1^{\mathrm{T}} \mathbf{u}_2^{\mathrm{T}} \ldots \mathbf{u}_{N_{\mathrm{fen}}}^{\mathrm{T}} \mid \boldsymbol{\alpha}_{10}^{\mathrm{T}} \boldsymbol{\alpha}_{11}^{\mathrm{T}} \ldots \boldsymbol{\alpha}_{1N_{\mathrm{pol}}}^{\mathrm{T}} \ldots \boldsymbol{\alpha}_{N_{fs}N_{\mathrm{pol}}}^{\mathrm{T}}], \tag{4}$$

where the displacement coefficients are $\mathbf{u}_I^{\mathrm{T}} = [\, u_I \quad v_I \,]$ and $\boldsymbol{\alpha}_{Im}^{\mathrm{T}} = [\, u_{Im} \quad v_{Im} \,]$, N_{fen} is the total number of assigned finite element nodes for displacement degrees of freedom in Ω_{FE} and $\Omega_{\mathrm{FE-FS}}$, and N_{pol} is the number of terms in the polynomials of the spheres used. To have a continuous displacement field, the finite element degrees of freedom on the boundary of $\Omega_{\mathrm{FE-FS}}$ with Ω_{FS} are not included (so that for the example in Fig. 1, $N_{\mathrm{fen}} = 6$, not including the nodes fixed on Γ_u). As a consequence, we cover all finite elements adjoining that boundary completely with spheres.

For the pure finite element subdomain $\Omega_{\mathrm{FE}}^{(k)}$, we use the conventional shape functions $h_I^{\mathrm{FE}}(\mathbf{x})$ [9]. In the pure finite sphere subdomain, considering the sphere I, the shape functions are $h_{Im}^{\mathrm{FS}}(\mathbf{x})$. The construction of these functions is achieved by multiplying the basic Shepard functions $\rho_I(\mathbf{x})$ with polynomial functions $p_m(\mathbf{x})$ to obtain $h_{Im}^{\mathrm{FS}}(\mathbf{x}) = \rho_I(\mathbf{x}) p_m(\mathbf{x})$, see [10]. The coupled subdomains $\Omega_{\mathrm{FE-FS}}^{(k)}$ have the shape functions $h_I^{\mathrm{FE-FS}}(\mathbf{x})$ corresponding to the finite element nodes and $h_{Im}^{\mathrm{FE-FS}}(\mathbf{x})$ corresponding to the finite sphere nodes. We discuss these functions below.

2.1. Principle of virtual work

The formulation is based on the following general variational statement for linear elastic problems [6,9]

$$\begin{aligned} &\text{Find} \quad \mathbf{u} \in H^1(\Omega) \\ &\text{such that} \int_\Omega \boldsymbol{\epsilon}^{\mathrm{T}}(\mathbf{v}) \mathbf{C} \boldsymbol{\epsilon}(\mathbf{u}) \, \mathrm{d}\Omega \\ &\qquad - \int_{\Gamma_u} [\boldsymbol{\epsilon}^{\mathrm{T}}(\mathbf{v}) \mathbf{C} \mathbf{N}^{\mathrm{T}} \mathbf{u} + \mathbf{v}^{\mathrm{T}} \mathbf{N} \mathbf{C} \boldsymbol{\epsilon}(\mathbf{u})] \, \mathrm{d}\Gamma \\ &\qquad = \int_\Omega \mathbf{v}^{\mathrm{T}} \mathbf{f}^B \, \mathrm{d}\Omega + \int_{\Gamma_f} \mathbf{v}^{\mathrm{T}} \mathbf{f}^s \, \mathrm{d}\Gamma \\ &\qquad - \int_{\Gamma_u} \boldsymbol{\epsilon}^{\mathrm{T}}(\mathbf{v}) \mathbf{C} \mathbf{N}^{\mathrm{T}} \mathbf{u}^s \, \mathrm{d}\Gamma \quad \forall \mathbf{v} \in H^1(\Omega), \end{aligned} \tag{5}$$

where $\boldsymbol{\epsilon}$ is the strain vector, $\mathbf{C}$ is the elasticity matrix, $\mathbf{u}$ is the unknown displacement field, $\mathbf{f}^s$ is the prescribed surface traction vector on the boundary Γ_f, $\mathbf{u}^s$ is the prescribed displacement vector on the boundary Γ_u, $\mathbf{f}^B$ is the applied body force vector and $H^1(\Omega)$ is the first order Hilbert space. To help enforcing the Dirichlet boundary conditions, a penalty term could also be added in Eq. (5) [9], but was not needed in our example solutions.

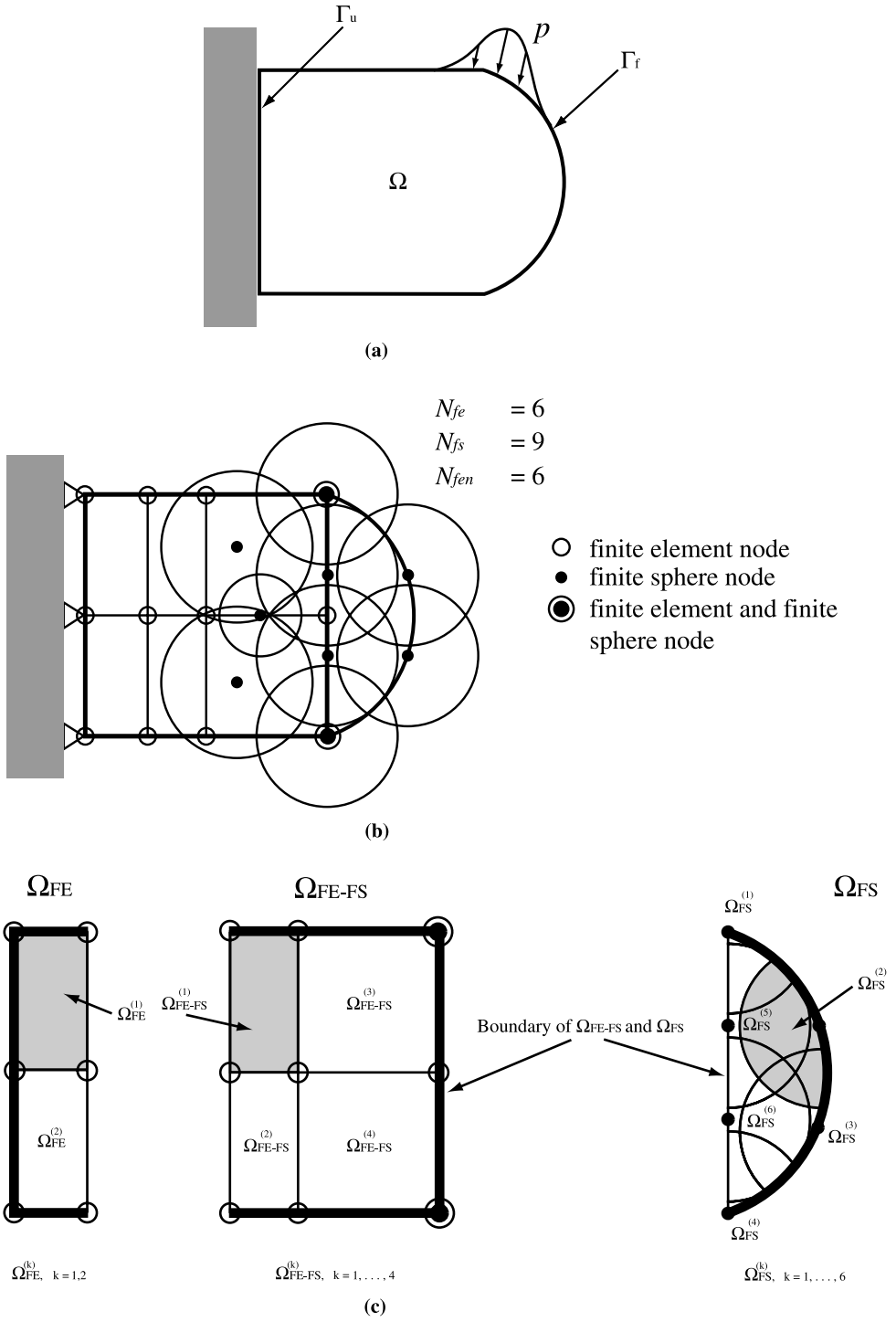

Fig. 1. Discretization of cantilever plate to illustrate coupling scheme: (a) structure considered and (b) finite elements and finite spheres discretizing the plate. We call Ω_{FE} the domain which does not have any overlap with finite spheres, $\Omega_{\mathrm{FE-FS}}$ the union of finite elements which have non-zero overlap with spheres, and Ω_{FS} the region which consists of spheres. (c) Individual computational domains over which we integrate numerically.

Considering two-dimensional analysis conditions the directional matrix $\mathbf{N}$ is defined as

$$\mathbf{N} = \begin{bmatrix} n_x & 0 & n_y \\ 0 & n_y & n_x \end{bmatrix}, \tag{6}$$

where n_x and n_y are the direction cosines of the outward unit normal vector.

Note that we use this variational statement for the complete analysis domain, but in the "pure" finite element domain (Ω_{FE}) the expression simplifies to the usual principle of virtual work [9].

2.2. Formulation in the "pure" finite element domain Ω_{FE}

In the domain Ω_{FE}, the finite elements do not overlap with finite spheres, and considering 4-node elements, the displacement field and strains in $\Omega_{\mathrm{FE}}^{(k)}$, k an element of $\mathscr{M}$, are those computed in the conventional finite element method [9]

$$\mathbf{u}_{\Omega_{\mathrm{FE}}}(\mathbf{x}) = \sum_{I=1}^{4} \mathbf{H}_I^{\mathrm{FE}}(\mathbf{x})\mathbf{u}_I, \tag{7}$$

$$\boldsymbol{\epsilon}_{\Omega_{\mathrm{FE}}}(\mathbf{x}) = \sum_{I=1}^{4} \mathbf{B}_I^{\mathrm{FE}}(\mathbf{x})\mathbf{u}_I, \tag{8}$$

where $\mathbf{u}_I^{\mathrm{T}} = [u_I \; v_I]$ and u_I and v_I are the x- and y-directional nodal displacements, respectively. The terms in the $\mathbf{H}_I^{\mathrm{FE}}$ and $\mathbf{B}_I^{\mathrm{FE}}$ matrices are obtained from the well-known finite element interpolation functions, $h_I(\mathbf{x})$. The complete formulation of the governing nodal equations is, for example, given in [9].

2.3. Formulation in the "pure" finite sphere domain Ω_{FS}

In the domain Ω_{FS} which we call the "pure" finite sphere domain, the displacements and strains for the subdomain $\Omega_{\mathrm{FS}}^{(k)}$, k a sphere of $\mathscr{S}$, are

$$\mathbf{u}_{\Omega_{\mathrm{FS}}}(\mathbf{x}) = \sum_{J=1}^{N_{\mathrm{spheres}}} \sum_{n\in\mathfrak{I}} \mathbf{H}_{Jn}^{\mathrm{FS}}(\mathbf{x})\boldsymbol{\alpha}_{Jn}, \tag{9}$$

$$\boldsymbol{\epsilon}_{\Omega_{\mathrm{FS}}}(\mathbf{x}) = \sum_{J=1}^{N_{\mathrm{spheres}}} \sum_{n\in\mathfrak{I}} \mathbf{B}_{Jn}^{\mathrm{FS}}(\mathbf{x})\boldsymbol{\alpha}_{Jn}, \tag{10}$$

where $\mathfrak{I}$ is an index set corresponding to the nth degree of freedom of the Jth sphere, $\boldsymbol{\alpha}_{Jn}^{\mathrm{T}} = [u_{Jn} \;\; v_{Jn}]$, $\mathrm{span}_{n=0,1,2}\{p_n(\mathbf{x})\} = \{1, x, y\}$ and N_{spheres} is the number of spheres located in the pure finite sphere domain Ω_{FS}. The formulation using these interpolations is given in Ref. [10].

2.4. Formulation in the coupled domain Ω_{FE-FS}

The displacement field in the subdomain $\Omega_{\mathrm{FE-FS}}^{(k)}$, k an element of $\mathscr{N}$, is given by the shape functions $h_I^{\mathrm{FE-FS}}(\mathbf{x})$ and $h_{Jn}^{\mathrm{FE-FS}}(\mathbf{x})$

$$u_{\Omega_{\mathrm{FE-FS}}}(\mathbf{x}) = \sum_{I\in\chi} h_I^{\mathrm{FE-FS}}(\mathbf{x})u_I + \sum_{J=1}^{\mathrm{nfs}} \sum_{n\in\mathfrak{I}} h_{Jn}^{\mathrm{FE-FS}}(\mathbf{x})u_{Jn}, \tag{11}$$

$$v_{\Omega_{\mathrm{FE-FS}}}(\mathbf{x}) = \sum_{I\in\chi} h_I^{\mathrm{FE-FS}}(\mathbf{x})v_I + \sum_{J=1}^{\mathrm{nfs}} \sum_{n\in\mathfrak{I}} h_{Jn}^{\mathrm{FE-FS}}(\mathbf{x})v_{Jn}, \tag{12}$$

where χ is the index set of assigned finite element nodes,

$$h_I^{\mathrm{FE-FS}}(\mathbf{x}) = \frac{h_I(\mathbf{x})}{W}, \tag{13}$$

$$h_{Jn}^{\mathrm{FE-FS}}(\mathbf{x}) = \rho_J^{\mathrm{FE-FS}}(\mathbf{x})p_n(\mathbf{x}), \tag{14}$$

$$\rho_J^{\mathrm{FE-FS}}(\mathbf{x}) = \frac{W_J(\mathbf{x})}{W} \tag{15}$$

and W is given by

$$W(\mathbf{x}) = \sum_{K=1}^{\mathrm{nfs}} W_K(\mathbf{x}) + \sum_{I\in\chi} h_I(\mathbf{x}). \tag{16}$$

Here 'nfs' is the number of finite spheres which have an intersection with $\Omega_{\mathrm{FE-FS}}^{(k)}$ and W_K is the weighting function corresponding to the finite sphere K. Of course, the displacement interpolations used satisfy the partition of unity principle [11]. Hence the rigid body modes can be represented.

The strains in the domain $\Omega_{\mathrm{FE-FS}}^{(k)}$ are

$$\epsilon_{xx}(\mathbf{x}) = \sum_{I\in\chi} h_{I,x}^{\mathrm{FE-FS}}(\mathbf{x})u_I + \sum_{J=1}^{\mathrm{nfs}} \sum_{n\in\mathfrak{I}} h_{Jn,x}^{\mathrm{FE-FS}}(\mathbf{x})u_{Jn}, \tag{17}$$

$$\epsilon_{yy}(\mathbf{x}) = \sum_{I\in\chi} h_{I,y}^{\mathrm{FE-FS}}(\mathbf{x})v_I + \sum_{J=1}^{\mathrm{nfs}} \sum_{n\in\mathfrak{I}} h_{Jn,y}^{\mathrm{FE-FS}}(\mathbf{x})v_{Jn}, \tag{18}$$

$$\gamma_{xy}(\mathbf{x}) = \sum_{I\in\chi} h_{I,y}^{\mathrm{FE-FS}}(\mathbf{x})u_I + \sum_{I\in\chi} h_{I,x}^{\mathrm{FE-FS}}(\mathbf{x})v_I + \sum_{J=1}^{\mathrm{nfs}} \sum_{n\in\mathfrak{I}} h_{Jn,y}^{\mathrm{FE-FS}}(\mathbf{x})u_{Jn} + \sum_{J=1}^{\mathrm{nfs}} \sum_{n\in\mathfrak{I}} h_{Jn,x}^{\mathrm{FE-FS}}(\mathbf{x})v_{Jn}. \tag{19}$$

In matrix form, the displacement and strain fields are

$$\mathbf{u}_{\Omega_{\mathrm{FE-FS}}}(\mathbf{x}) = \sum_{I\in\chi} \mathbf{H}_I^{\mathrm{FE-FS}}(\mathbf{x})\mathbf{u}_I + \sum_{J=1}^{\mathrm{nfs}} \sum_{n\in\mathfrak{I}} \mathbf{H}_{Jn}^{\mathrm{FE-FS}}(\mathbf{x})\boldsymbol{\alpha}_{Jn}, \tag{20}$$

$$\boldsymbol{\epsilon}_{\Omega_{\text{FE–FS}}}(\mathbf{x}) = \sum_{I\in\chi} \mathbf{B}_I^{\text{FE–FS}}(\mathbf{x})\mathbf{u}_I + \sum_{J=1}^{\text{nfs}} \sum_{n\in\mathfrak{I}} \mathbf{B}_{Jn}^{\text{FE–FS}}(\mathbf{x})\boldsymbol{\alpha}_{Jn}. \tag{21}$$

The displacement matrix $\mathbf{H}_I^{\text{FE–FS}}(\mathbf{x})$ and strain–displacement matrix $\mathbf{B}_I^{\text{FE–FS}}(\mathbf{x})$ for the finite element node I are

$$\mathbf{H}_I^{\text{FE–FS}}(\mathbf{x}) = \begin{bmatrix} h_I^{\text{FE–FS}}(\mathbf{x}) & 0 \\ 0 & h_I^{\text{FE–FS}}(\mathbf{x}) \end{bmatrix}, \tag{22}$$

$$\mathbf{B}_I^{\text{FE–FS}}(\mathbf{x}) = \begin{bmatrix} h_{I,x}^{\text{FE–FS}}(\mathbf{x}) & 0 \\ 0 & h_{I,y}^{\text{FE–FS}}(\mathbf{x}) \\ h_{I,y}^{\text{FE–FS}}(\mathbf{x}) & h_{I,x}^{\text{FE–FS}}(\mathbf{x}) \end{bmatrix} \tag{23}$$

and the displacement matrix $\mathbf{H}_{Jn}^{\text{FE–FS}}(\mathbf{x})$ and strain–displacement matrix $\mathbf{B}_{Jn}^{\text{FE–FS}}(\mathbf{x})$ for the finite sphere node J with degree of freedom n are

$$\mathbf{H}_{Jn}^{\text{FE–FS}}(\mathbf{x}) = \begin{bmatrix} h_{Jn}^{\text{FE–FS}}(\mathbf{x}) & 0 \\ 0 & h_{Jn}^{\text{FE–FS}}(\mathbf{x}) \end{bmatrix}, \tag{24}$$

$$\mathbf{B}_{Jn}^{\text{FE–FS}}(\mathbf{x}) = \begin{bmatrix} h_{Jn,x}^{\text{FE–FS}}(\mathbf{x}) & 0 \\ 0 & h_{Jn,y}^{\text{FE–FS}}(\mathbf{x}) \\ h_{Jn,y}^{\text{FE–FS}}(\mathbf{x}) & h_{Jn,x}^{\text{FE–FS}}(\mathbf{x}) \end{bmatrix}. \tag{25}$$

Here the x- and y-derivatives of $h_J^{\text{FE–FS}}(\mathbf{x})$ are

$$h_{J,x}^{\text{FE–FS}}(\mathbf{x}) = \left[h_{J,x} - \frac{h_J}{W}W_{,x}\right]\frac{1}{W}, \tag{26}$$

$$h_{J,y}^{\text{FE–FS}}(\mathbf{x}) = \left[h_{J,y} - \frac{h_J}{W}W_{,y}\right]\frac{1}{W}. \tag{27}$$

Also

$$h_{Jn,x}^{\text{FE–FS}}(\mathbf{x}) = \rho_{J,x}^{\text{FE–FS}}(\mathbf{x})p_n + \rho_J^{\text{FE–FS}}(\mathbf{x})p_{n,x}, \tag{28}$$

$$h_{Jn,y}^{\text{FE–FS}}(\mathbf{x}) = \rho_{J,y}^{\text{FE–FS}}(\mathbf{x})p_n + \rho_J^{\text{FE–FS}}(\mathbf{x})p_{n,y}, \tag{29}$$

where

$$\rho_{J,x}^{\text{FE–FS}}(\mathbf{x}) = \left[W_{J,x} - \frac{W_J}{W}W_{,x}\right]\frac{1}{W}, \tag{30}$$

$$\rho_{J,y}^{\text{FE–FS}}(\mathbf{x}) = \left[W_{J,y} - \frac{W_J}{W}W_{,y}\right]\frac{1}{W}. \tag{31}$$

With these interpolation functions given, we can directly substitute into the virtual work equation, Eq. (5), and obtain as usual all governing equations for each subdomain $\Omega_{\text{FE–FS}}^{(k)}$, see Ref. [9]. For example, the individual stiffness values are obtained as

$$\mathbf{K}_{IJ}^{\text{FE–FS}} = \int_{\Omega_{\text{FE–FS}}^{(k)}} \mathbf{B}_I^{FE-FS^{\mathrm{T}}}(\mathbf{x})\mathbf{C}\mathbf{B}_J^{\text{FE–FS}}(\mathbf{x})\,\mathrm{d}\Omega, \tag{32}$$

$$\mathbf{K}_{IJn}^{\text{FE–FS}} = \int_{\Omega_{\text{FE–FS}}^{(k)}} \mathbf{B}_I^{FE-FS^{\mathrm{T}}}(\mathbf{x})\mathbf{C}\mathbf{B}_{Jn}^{\text{FE–FS}}(\mathbf{x})\,\mathrm{d}\Omega, \tag{33}$$

$$\mathbf{K}_{ImJ}^{\text{FE–FS}} = \int_{\Omega_{\text{FE–FS}}^{(k)}} \mathbf{B}_{Im}^{FE-FS^{\mathrm{T}}}(\mathbf{x})\mathbf{C}\mathbf{B}_J^{\text{FE–FS}}(\mathbf{x})\,\mathrm{d}\Omega, \tag{34}$$

$$\mathbf{K}_{ImJn}^{\text{FE–FS}} = \int_{\Omega_{\text{FE–FS}}^{(k)}} \mathbf{B}_{Im}^{FE-FS^{\mathrm{T}}}(\mathbf{x})\mathbf{C}\mathbf{B}_{Jn}^{\text{FE–FS}}(\mathbf{x})\,\mathrm{d}\Omega. \tag{35}$$

2.5. Assemblage of complete stiffness matrix and force vector for Ω

The first term in Eq. (5) gives

$$\int_\Omega \boldsymbol{\epsilon}^{\mathrm{T}}\mathbf{C}\boldsymbol{\epsilon}\,\mathrm{d}\Omega = \int_{\Omega_{\text{FE}}} \boldsymbol{\epsilon}^{\mathrm{T}}\mathbf{C}\boldsymbol{\epsilon}\,\mathrm{d}\Omega + \int_{\Omega_{\text{FS}}} \boldsymbol{\epsilon}^{\mathrm{T}}\mathbf{C}\boldsymbol{\epsilon}\,\mathrm{d}\Omega + \int_{\Omega_{\text{FE–FS}}} \boldsymbol{\epsilon}^{\mathrm{T}}\mathbf{C}\boldsymbol{\epsilon}\,\mathrm{d}\Omega. \tag{36}$$

By substituting from Eqs. (8), (10) and (21) we obtain the total stiffness matrix for the assemblage

$$\mathbf{K} = \left\{\sum_{k\in\mathscr{M}} \int_{\Omega_{\text{FE}}^{(k)}} \mathbf{B}_{\text{FE}}^{(k)^{\mathrm{T}}}\mathbf{C}\mathbf{B}_{\text{FE}}^{(k)}\,\mathrm{d}\Omega^{(k)}\right\} + \left\{\sum_{k\in\mathscr{P}} \int_{\Omega_{\text{FS}}^{(k)}} \mathbf{B}_{\text{FS}}^{(k)^{\mathrm{T}}}\mathbf{C}\mathbf{B}_{\text{FS}}^{(k)}\,\mathrm{d}\Omega^{(k)}\right\} + \left\{\sum_{k\in\mathscr{N}} \int_{\Omega_{\text{FE–FS}}^{(k)}} \mathbf{B}_{\text{FE–FS}}^{(k)^{\mathrm{T}}}\mathbf{C}\mathbf{B}_{\text{FE–FS}}^{(k)}\,\mathrm{d}\Omega^{(k)}\right\} \tag{37}$$

and similarly we obtain the total force vector. Hence, the equation corresponding to the finite element node I is

$$\sum_{J\in\mathscr{L}} \mathbf{K}_{IJ}\mathbf{u}_J + \sum_{J\in\mathscr{K}}\sum_{n\in\mathfrak{I}} \mathbf{K}_{IJn}\boldsymbol{\alpha}_{Jn} = \mathbf{f}_I + \hat{\mathbf{f}}_I \tag{38}$$

and the equation corresponding to the finite sphere node I with degree of freedom m is

$$\sum_{J\in\mathscr{L}} \mathbf{K}_{ImJ}\mathbf{u}_J + \sum_{J\in\mathscr{K}}\sum_{n\in\mathfrak{I}} \mathbf{K}_{ImJn}\boldsymbol{\alpha}_{Jn} = \mathbf{f}_{Im} + \hat{\mathbf{f}}_{Im}, \tag{39}$$

where $\mathscr{L}$ is the index of finite element nodes and $\mathscr{K}$ is the index of finite sphere nodes. In Eqs. (38) and (39), $\mathbf{f}_I$, $\hat{\mathbf{f}}_I$, $\mathbf{f}_{Im}$ and $\hat{\mathbf{f}}_{Im}$ correspond to the applied body forces, surface tractions and imposed displacement boundary conditions, see Refs. [9,10] where also the numerical integration used is presented.

3. Enriching the finite element displacement functions

We can also use finite spheres to simply enrich the traditional finite element displacement interpolations, as illustrated in Fig. 2. Since the finite element displacement functions satisfy the partition of unity principle already, it is possible to add spheres adaptively. Then the

equations for the shape functions in $\Omega_{\text{FE–FS}}$ are of the form

$$h_I^{\text{FE–FS}}(\mathbf{x}) = h_I, \tag{40}$$

$$\rho_I^{\text{FE–FS}}(\mathbf{x}) = W_I, \tag{41}$$

$$h_{Im}^{\text{FE–FS}}(\mathbf{x}) = \rho_I^{\text{FE–FS}}(\mathbf{x}) p_m(\mathbf{x}). \tag{42}$$

And the displacement field in the domain $\Omega_{\text{FE–FS}}^{(k)}$ is

$$u_{\Omega_{\text{FE–FS}}}^{(k)}(\mathbf{x}) = \sum_{I=1}^{4} h_I^{\text{FE–FS}}(\mathbf{x}) u_I + \sum_{J=1}^{\text{nfs}} \sum_{n\in\mathfrak{I}} h_{Jn}^{\text{FE–FS}}(\mathbf{x}) u_{Jn}, \tag{43}$$

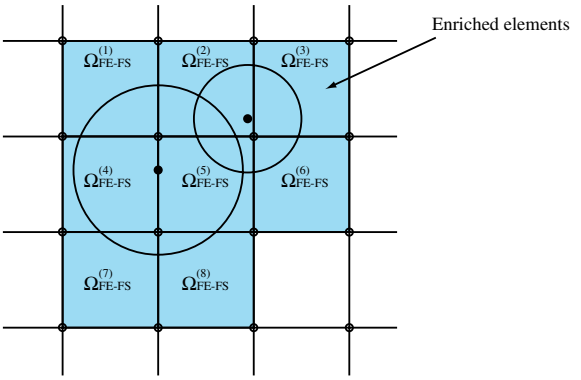

Fig. 2. Enriching a finite element discretization with finite spheres: we call Ω_{FE} the domain which is not enriched with finite spheres, and $\Omega_{\text{FE–FS}}$, the domain of finite elements enriched with spheres.

$$v_{\Omega_{\text{FE–FS}}}^{(k)}(\mathbf{x}) = \sum_{I=1}^{4} h_I^{\text{FE–FS}}(\mathbf{x}) v_I + \sum_{J=1}^{\text{nfs}} \sum_{n\in\mathfrak{I}} h_{Jn}^{\text{FE–FS}}(\mathbf{x}) v_{Jn}. \tag{44}$$

The total stiffness matrix is obtained by summing the contributions from all subdomains

$$\mathbf{K} = \left\{ \sum_{k\in\mathscr{M}} \int_{\Omega_{\text{FE}}^{(k)}} \mathbf{B}_{\text{FE}}^{(k)\text{T}} \mathbf{C} \mathbf{B}_{\text{FE}}^{(k)} \, \mathrm{d}\Omega^{(k)} \right\} + \left\{ \sum_{k\in\mathscr{N}} \int_{\Omega_{\text{FE–FS}}^{(k)}} \mathbf{B}_{\text{FE–FS}}^{(k)\text{T}} \mathbf{C} \mathbf{B}_{\text{FE–FS}}^{(k)} \, \mathrm{d}\Omega^{(k)} \right\}, \tag{45}$$

where, again, $\mathscr{M}$ is the index of the finite element subdomains and $\mathscr{N}$ is the index of the subdomains enriched with finite spheres.

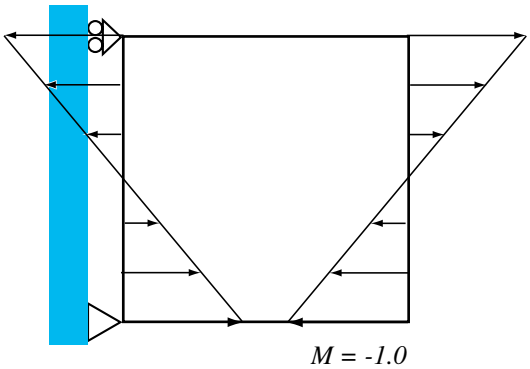

Fig. 3. Loading condition for bending test: a linear pressure distribution resulting in a unit moment load. Plane strain conditions, Young's modulus $E = 100$, Poisson's ratio $\nu = 0.30$.

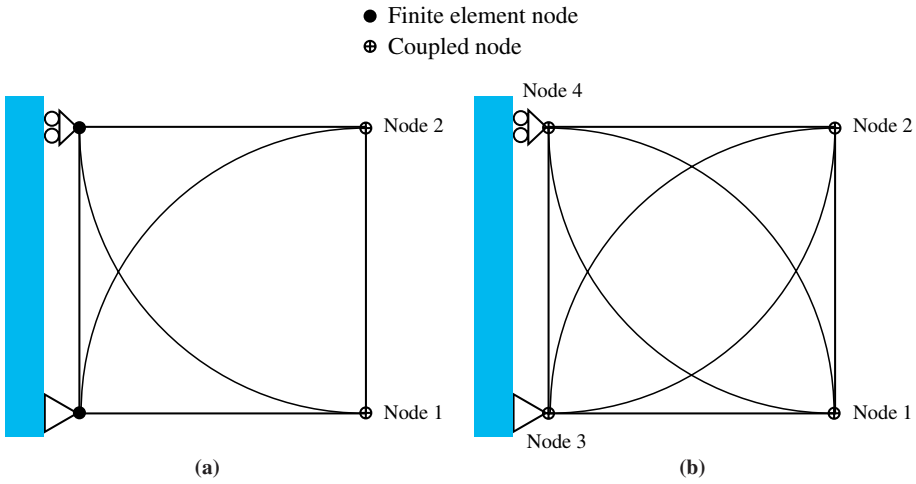

Fig. 4. Sphere arrangements on a 4-node finite element. (a) Scheme A: two spheres are located with centers at nodes 1 and 2. (b) Scheme B: four spheres are located, each with its center at a finite element node.

4. Example solutions

We present in this section various example solutions to illustrate the use of finite element discretizations coupled to and enriched with finite spheres.

4.1. Bending of cantilever

As is well-known, a single 4-node displacement-based element can represent exactly the constant stress conditions and so, of course, does any patch enriched with finite spheres. However, the 4-node element represents a uniform bending condition only very poorly [9].

We consider, in this example, the cantilever shown in Fig. 3 subjected to the constant bending moment. The structure is analyzed with the finite element/finite sphere discretizations denoted as schemes A and B shown in Fig. 4. Fig. 5 summarizes the refinements used in the solutions. Figs. 6 and 7 show the convergence of the solutions obtained, in terms of the strain energy per unit length of beam. We can see that the use of the finite spheres significantly increases the accuracy of the solution, and, as expected, the use of scheme B results in better solution accuracy than the use of scheme A.

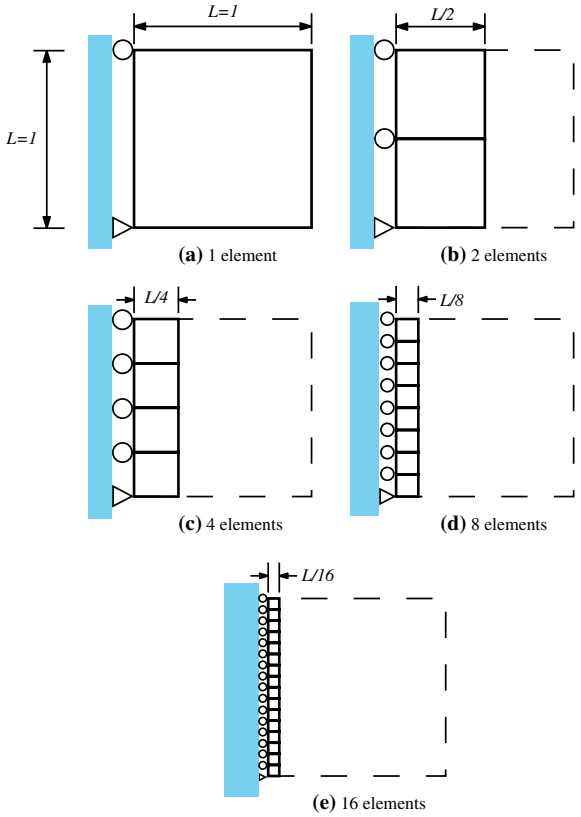

Fig. 5. Element refinements used in convergence study.

4.2. Analysis of a plate with a hole

We consider a square plate with a hole as shown in Fig. 8. Using $a/b = 0.1$, the stress concentration factor is 3.08. An accurate solution can of course be obtained with a sufficiently fine mesh of traditional finite elements.

To use the enriching scheme, we placed two spheres on the top and bottom of the hole, respectively, as shown with a typical finite element discretization in Fig. 9. The comparison of the maximum σ_{xx} stress obtained using the mesh in Fig. 9 and uniformly refining this mesh is summarized in Table 1. As listed in Table 1, the finite element method using 4-node elements yields

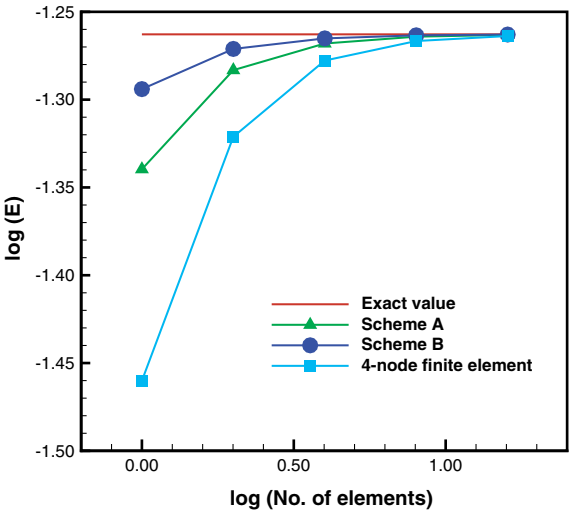

Fig. 6. Strain energy comparison with 4-node finite elements.

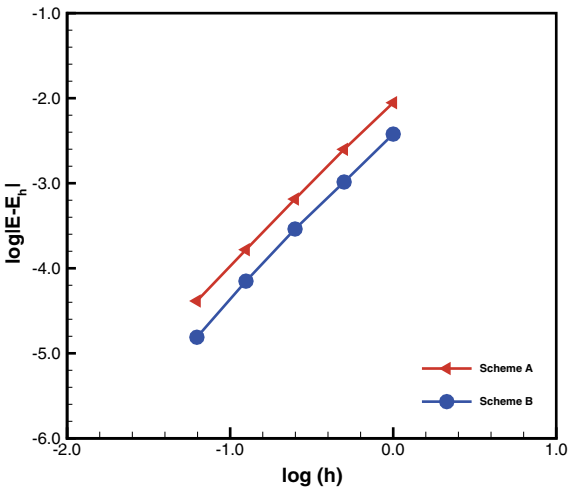

Fig. 7. Convergence curves with different sphere allocations shown in Fig. 4.

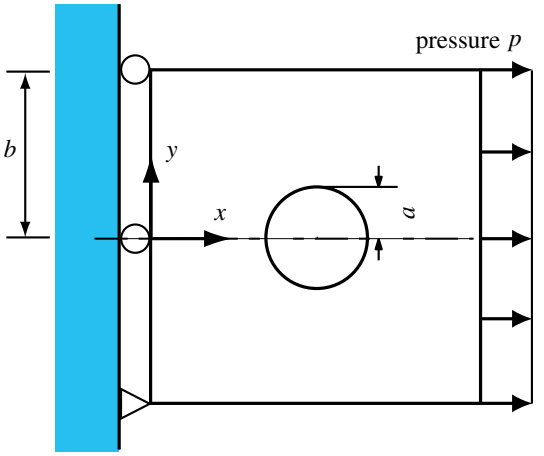

Fig. 8. Geometry of a square plate with a hole in the middle of the plate. Young's modulus $E = 100$, Poisson's ratio $\nu = 0.30$, $p = 1$.

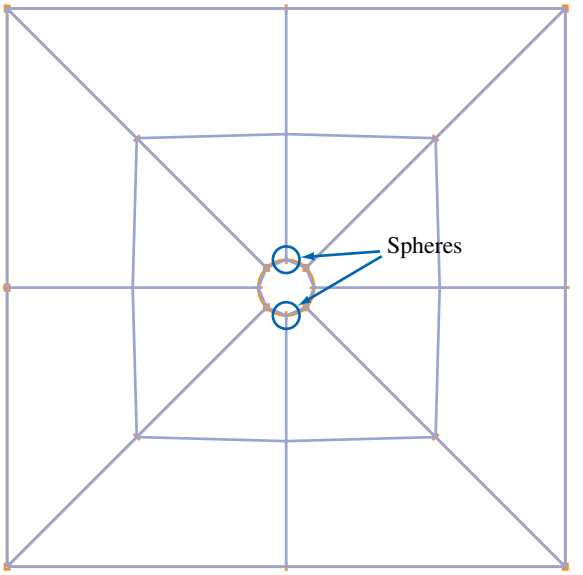

Fig. 9. Sixteen 4-node element mesh and placement of the finite spheres for enrichment.

the largest solution error and then using the enriching scheme gives better results than the use of pure 9-node elements.

To illustrate the coupling scheme, we adopt a pure sphere domain coupled to a pure finite element domain, and the discretization shown in Fig. 10. With this discretization the maximum σ_{xx} stress is 2.736.

4.3. Plate with a crack

We consider a plate in plane strain conditions containing a sharp crack [12]. The plate is subjected to pressure as shown in Fig. 11. For the analysis we use 4-node elements in uniform meshes. We also use the same meshes but enriched with a single sphere of radius 0.1 at the crack tip.

Fig. 12 and Table 2 give the results obtained for the normal stress in the plate. We see that the stress prediction is much improved by adding the sphere to the finite element discretization.

Table 1
Comparison of maximum σ_{xx} stress in the plate with a hole shown in Fig. 8 when using the enrichment scheme

No. of elements for full plate	FEM (4-nodes)	FEM (9-nodes)	Enriching scheme with 4-node elements	Accurate value
16	1.455	1.937	2.464	
64	1.878	2.388	2.649	
256	2.383	2.785	2.957	3.08

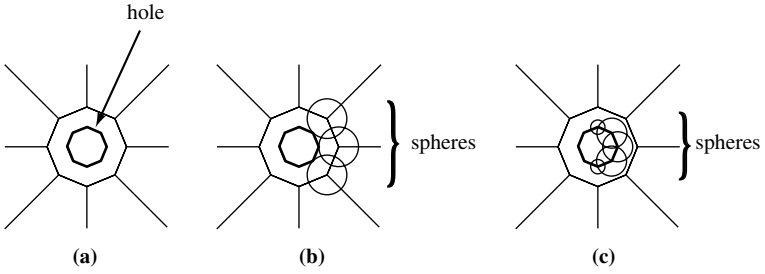

Fig. 10. Discretization used near the hole with 16 4-node finite element mesh. (a) Finite elements and (b) spheres which have coupling with the finite elements; (c) spheres which do not have coupling with the finite elements (Not shown are the additional spheres to completely cover the finite elements adjacent to the hole.).

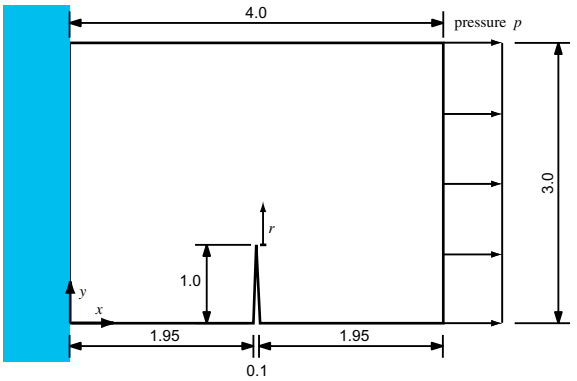

Fig. 11. A plate with a sharp crack. Young's modulus $E = 100$, Poisson's ratio $v = 0.30$. The plate is in plane strain conditions, $p = 1$.

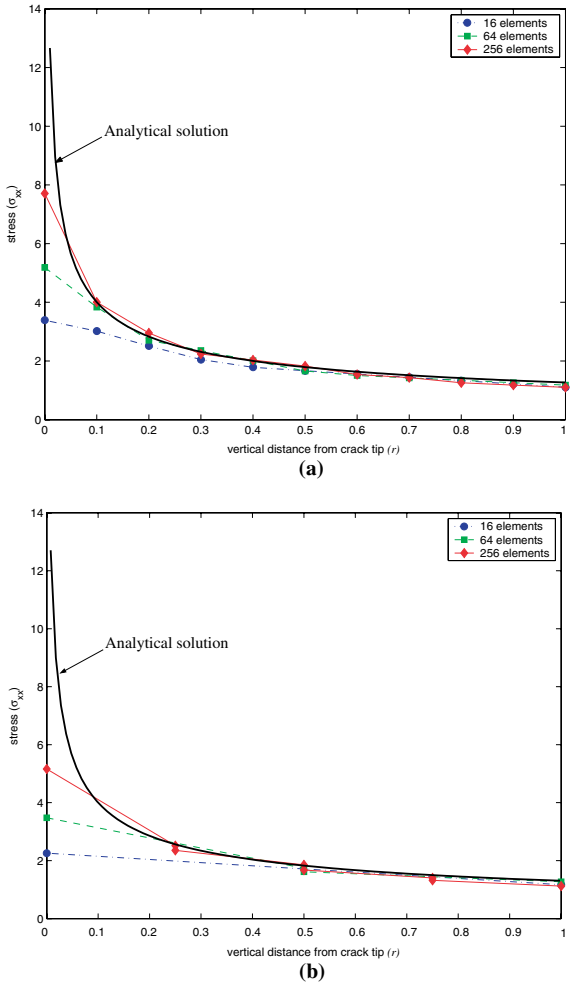

Fig. 12. Analysis of plate with a crack. Solution of σ_{xx} as a function of r: (a) using the enriching scheme and (b) not using the enriching scheme.

Table 2
Comparison of maximum σ_{xx} stress on the crack tip

No. of elements	FEM (4-nodes)	Enriching scheme
16	2.330	3.390
64	3.518	5.188
256	5.203	7.710

5. Concluding remarks

The objective of this paper was to propose a coupling scheme and an enriching scheme which enable to use finite elements and finite spheres simultaneously. With these two fully coupled discretization schemes, more flexibility in performing analysis in an effective way is available.

The coupling scheme, using the traditional finite element discretization for some domains and the finite sphere discretization for adjoining domains, imposes full displacement compatibility in the analysis region. The scheme is based on a straight-forward application of the partition of unity principle. However, further studies are needed to fully identify the effectiveness of this scheme because the numerical integration is still rather expensive for the coupled domain and the finite sphere domain, and the proper placing of spheres (the number of spheres and their radii) is important.

The enriching scheme using finite spheres on finite element discretizations simply corresponds to enriching the space of assumed displacements. However, the key for practical purposes is that the spheres can be placed anywhere on the underlying finite element mesh, and hence can be used adaptively to enrich a traditional finite element discretization.

The proposed procedures represent a generalization of the traditional finite element method. While the methods have been used in this paper only for linear two-dimensional analysis, and using only specific low-order finite element and finite sphere discretizations, the real power of the methods might be harnessed in the analysis of large deformation and multi-physics problems, such as fluid flows with structural interactions. Some inherent difficulties arising in the use of the traditional finite element methods due to mesh distortions can be avoided by using the methods proposed in this paper, but as mentioned already the effectiveness of the schemes for such solutions must still be studied.

References

[1] Bathe KJ, editor. Computational fluid and solid mechanics. Elsevier; 2001.
[2] Bathe KJ, editor. Computational fluid and solid mechanics 2003. Elsevier; 2003.
[3] Liu GR, Gu YT. Coupling of element free Galerkin and hybrid boundary element methods using modified

variational formulation. Computat Mech 2000;26: 166–73.
[4] Liu GR, Gu YT. Meshless local Petrov–Galerkin (MLPG) method in combination with finite element and boundary element approaches. Computat Mech 2000;26:536–46.
[5] Karutz H, Chudoba R, Krätzig WB. Automatic adaptive generation of a coupled finite element/element-free Galerkin discretization. Finite Elem Anal Design 2002;38: 1075–91.
[6] De S, Bathe KJ. The method of finite spheres with improved numerical integration. Comput Struct 2001; 79:2183–96.
[7] Hong JW, Bathe KJ. On analytical transformations for efficiency improvements in the method of finite spheres. In: Bathe KJ, editor. Computational fluid and solid mechanics 2003. Elsevier; 2003. p. 1990–4.
[8] De S, Hong JW, Bathe KJ. On the method of finite spheres in applications: towards the use with ADINA and in a surgical simulator. Computat Mech 2003;31:27–37.
[9] Bathe KJ. Finite element procedures. Upper Saddle River, NJ: Prentice Hall; 1996.
[10] De S, Bathe KJ. The method of finite spheres. Computat Mech 2000;25:329–45.
[11] Yosida K. Functional analysis. Berlin, Heidelberg: Springer; 1995.
[12] Anderson TL. Fracture mechanics: fundamentals and applications. Boca Raton, FL: CRC Press; 1991.